

RESEARCH PAPER

## Synthesis and biological activity of siRNA and Etoposide with magnetic nanoparticles on drug resistance model MCF-7 cells: Molecular docking study with MRP1 enzyme

Serap Yalcin <sup>1\*</sup>, Ufuk Gündüz <sup>2</sup>

<sup>1</sup>Department of Molecular Biology and Genetics, Kirsehir Ahi Evran University, Kirsehir, Turkey

<sup>2</sup>Department of Biology, Middle East Technical University, Ankara, Turkey

### ABSTRACT

**Objective(s):** In this work, MRP-1 (Multidrug resistance-associated protein 1) gene expression levels and anticancer activity of siRNA and Etoposide loaded Poly-hydroxybutyrate (PHB) coated magnetic nanoparticles (MNPs) was studied on MCF-7/Sensitive and MCF-7/1000Etoposide resistance cells. For this purpose, PHB covered iron oxide-based magnetic nanoparticles (PHB-MNPs) were prepared by coprecipitation. We used magnetic nanoparticles because they include highly targeted to tumors in vivo cancer therapy.

**Materials and Methods:** Etoposide, anti-cancer drug, was loaded onto the PHB-MNPs. The in vitro cytotoxicity analysis of siRNA and Etoposide-loaded PHB-MNPs was applied on cancer cells. The expression levels of MRP1 related to drug resistance were shown using qRT-PCR. In the present study, we also investigated whether nanoparticle system could be a potential anticancer drug target with molecular docking analyses.

**Results:** The IC50 values of Etoposide on MCF-7/sensitive and MCF-7/1000Eto resistance cells were identified as 50,6 µM and 135,7 µM, respectively. IC50 values of siRNA and Etoposide loaded PHB coated magnetic nanoparticles were determined as 10,18 µM and 39,21 µM on MCF-7 and MCF-7/1000 Eto cells, respectively. According to the gene expression results, MRP1 expression was 4 fold upregulated in MCF-7/1000Eto cells. However, it was about 3 fold downregulated due to the application of siRNA-Etoposide loaded magnetic nanoparticles.

**Conclusion:** According to the docking results, nanoparticle system may be a drug active substance with obtained results. The results of this study demonstrated that siRNA and Etoposide loaded PHB covered iron oxide based magnetic nanoparticles can be a potential targeted therapeutic agent to overcome drug resistance.

**Keywords:** Anticancer effect, Breast Cancer, Etoposide, , Molecular docking, PHB coated magnetic nanoparticles, siRNA

### How to cite this article

Yalcin S, Gündüz U. Synthesis and biological activity of siRNA and Etoposide with magnetic nanoparticles on drug resistance model MCF-7 cells: Molecular docking study with MRP1 enzyme. *Nanomed J.* 2021; 8(2): 98-105.

DOI: [10.22038/nmj.2021.08.002](https://doi.org/10.22038/nmj.2021.08.002)

### INTRODUCTION

Etoposide (4'- reduction reactions [2,3]. In addition, Anti-cancer drug has a short biological half-life (3.6 hours). Furthermore, dimethyl-epipodophyllotoxin, VP16), is a lipophilic drug used in the treatment of different malignancies [1,2]. Etoposide is a topoisomerase-II inhibitor and plays activation of oxidation- the oral bioavailability of Etoposide is variable, ranging from 24–74 % [4,5].

The cellular uptake of anticancer drugs like etoposide with nanoparticles has been investigated using various methods [6]. The nano-based systems are capable to be drug reservoirs and drug concentration could be enhanced significantly after being taken inside tumor cells [7,8]. It has been reported that magnetic nanoparticles have boosted efficiency, reduced side effect and overcome the multidrug resistance (MDR) of the cancer cells in vitro and in vivo studies [9,10].

Currently, the different nanocarrier systems have designed including polymers, lipids, micelles,

\* Corresponding Author Email: [syalcin@ahievran.edu.tr](mailto:syalcin@ahievran.edu.tr)/[serapyalcin1982@gmail.com](mailto:serapyalcin1982@gmail.com)

Note. This manuscript was submitted on October 3, 2020; approved on January 15, 2021

etc. for increased drug efficiency in cancer therapy [11,12]. However, some nano-based systems such as liposomes, nanotubes can lead to undesirable side effects, due to fast degradation, toxic effect on healthy cells, crystallization properties [13,14].

Up to now, various nanoparticle formulations loading/conjugating etoposide were synthesized in polymeric nanosystems [15-24]. Unfortunately, the most complex designed and built from nanoparticles has an important disadvantage since nanoparticles were synthesized in solutions containing different organic solvents. These toxic materials are hazardous to humans health, and they have serious limitations for biomedical applications.

Magnetic nanoparticles (MNPs) are important therapeutic agents having a wide range of applications including MRI (magnetic resonance imaging) and cancer therapy. The targeted of MNPs are focus of interest in medicinal studies because they may be used for detection and therapy of various diseases such as cancer. These characteristics of MNPs lead to the way for diagnosis of tumors, chemotherapeutic monitoring, and simultaneous prognosis of treatment [10, 24].

The aim of this work was to (i) prepare and characterize a non-toxic PHB coated magnetic nanoparticles delivering the anticancer drug Etoposide and anti MRP1 siRNA, (ii) study the internalization and cytotoxicity of the siRNA and Etoposide loaded PHB coated magnetic nanoparticles, (iii) evaluate for the regulation of MRP1 gene activity in the Etoposide sensitive and resistant breast cancer cell line by Real-Time PCR techniques and (iv) whether drug loaded magnetic nanoparticles would inhibit MRP-1 protein with molecular docking analyses.

## MATERIALS AND METHODS

### ***Production of Etoposide loaded PHB-MNPs***

PHB-covered iron oxide-based magnetic iron oxide nanoparticles (PHB-MNPs) were synthesized by the coprecipitation of iron (II) chloride tetrahydrate and iron (III) chloride hexahydrate salts in the presence of PHB with some changes of Xiong et al. [23, 24]. Crystal structures of PHB-MNPs were found by XRD. The chemical groups of PHB-MNPs and Etoposide loaded PHB-MNPs were analyzed using the FTIR. The sizes and morphological features were shown by TEM images. The information about the volatile

compounds of the PHB-MNPs have been ensured by thermal gravimetric analysis (TGA), the hydrodynamic sizes were analysed by Dynamic light scattering(DLS) and magnetic properties were identified by VSM analyses [24].

### ***siRNA and Etoposide loading on PHB-MNPs***

The PHB-MNPs were synthesized according to the in situ synthesis method [24]. Polyethyleneimine (PEIs) create noncovalent complexes with nucleic acids and drugs and they have a positively charged. This structure causes protecting siRNAs from degradation, and lysosomal escape into the cytoplasm. PHB-MNPs solution (20 mg/mL) was mixed with an aqueous PEI solution (5 mg/mL).

The anticancer drug Etoposide was dissolved in PBS (pH 7.4), in various Etoposide concentrations (10, 50, 100, 150, 200 and 250 ug/mL). Etoposide and PHB-MNPs was turned for 24 hours in a light sensitive tube. Etoposide-PHB-MNPs were separated from the supernatant by magnetic separation.

For the preparation of siRNA-Etoposide loaded PHB-MNPs, PHB-MNPs was diluted at different N/P ratios and mixed with an equal volume of siRNA solution (2 pmol/ $\mu$ L) (Target sequences were: GCUGGUAGCCCUAGUGUGU for MRP1) [25] and then was vortexed for 20 s at room temperature. PHB-MNPs/siRNA to the mixture were loaded onto 1 % agarose gels and run with Tris-acetate running buffer at 160 V for 60 min. The retardation of siRNA was monitorized with ethidium bromide staining and photographed under BIORAD-DNA gel image analyzer. The loading or binding of maximum Etoposide concentration to the PHB-MNPs was approved by FTIR analysis.

### ***In vitro Etoposide Release and Stability of Etoposide from PHB-MNPs***

In vitro, Etoposide release of PHB-MNPs was determined in different solutions. The Etoposide loaded PHB-MNPs were dispersed in PBS (pH 7.4) and acetate buffer with (pH 4.1). The release of Etoposide (150 and 200 mg/mL) from PHB-MNPs was determined in up to 70 hours. The amount of released Etoposide was quantified solution at 280 nm by a UV spectrophotometer. Stabilities of Etoposide-PHB-MNPs were analysed in buffer (pH 7.4) at 37°C for up to 8 weeks. The stabilities of Etoposide were adjusted as the absorbance values at 280 nm by a UV spectrophotometer(BIOTEK).

### Cellular internalization of nanoparticles

siRNA-Etoposide-loaded PHB-MNPs were incubated at 37°C with drug sensitive and resistant cells in 6-well plates. After the cells treated with nanoparticles, were washed with PBS and the images of the cells were taken by inverted microscopy (BAB, Turkey).

### Cytotoxicity of nanoparticles

The sensitive cells was obtained from SAP Institute (Ankara, Turkey), and 1-mM Etoposide-resistant MCF-7 cell line, was developed by Kaplan and Gunduz, [26] were used. MCF-7/S and MCF-7/ETO cells were cultured in RPMI-1640 and 10% fetal bovine serum (FBS, Biological Industries, USA) and 1% gentamicin sulfate solution. The cell proliferation assay was taken by Biological Industries (Israel Beit Haemek LTD). The cytotoxic effects of siRNA-Etoposide-PHB-MNPs on Etoposide sensitive and resistance cells were evaluated by means of the XTT Cell Proliferation assay according to the manufacturer's instructions.

### Expression of MRP1 gene

The cancer cells were seeded in 6 well plates in RPMI-1640 media. After this, the cells were treated with free Etoposide, Etoposide loaded PHB-MNPs, siRNA-Etoposide loaded PHB-MNPs solutions, without any medium changes. IC50 values were calculated using the XTT assay, these values were applied to the cells. After incubation, cells were collected into High Pure RNA isolation reagent (Roche Life Sciences, USA). The RNA quality and quantity were determined by Nanodrop (OPTIZEN, Mecasys, Korea). cDNA was synthesized by using random hexamer primers and they were used as a template in quantitative PCR. The effect of siRNA-Etoposide loaded PHB-MNPs on MRP1 gene expressions were investigated from treated and non-treated cells. Fold changes of gene expression values after treatment was calculated by  $\Delta\Delta CT$  method and standardized with two housekeeping genes ( $\beta$ -ACTIN and GAPDH) [27].

### Molecular docking study

Molecular docking calculations was done using via Lamarckian Generic Algorithm [28] in Autodock Vina [29]. Molecular docking study were performed the crystal structure of human MRP1 protein (PDB code: 2CBZ)[30] which was obtained from the Protein Data Bank (PDB) database (<https://www.rcsb.org>). 3D structure

of nanoparticles was drawn with GAUSSIAN 09 program [31] and all obtained protein-ligand interaction results were visualized in the Molecular Viewer 2.5 (Molegro Molecular viewer free software, <http://www.molegro.com>) [32].

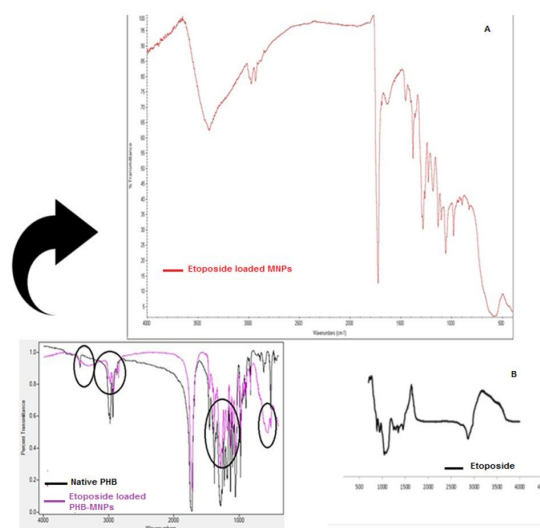


Fig 1. FTIR spectra of Etoposide loaded PHB-MNPs and native PHB (A), The ATR spectra of Etoposide(B)

## RESULTS

We previously published the synthesis method of PHB coated MNPs [24]. PHB covered MNPs were optimized by adjusting the temperature in the range of 20°C - 90°C. Crystal structures of pure iron oxides were obtained at 90°C. The characterization of MNPs was analyzed by FTIR, TEM, TGA and VSM analyses [24].

The ATR spectra of free etoposide and the FTIR spectra Etoposide loaded PHB coated MNPs were also shown in Fig 1. Peaks at 3400cm-1 and 1576 cm-1 were indicated that Etoposide was loaded to PHB coated MNPs.

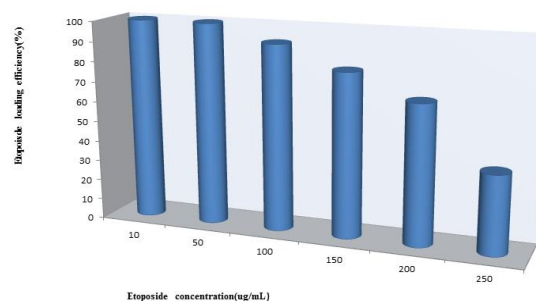


Fig 2. Loading efficiencies of different concentrations of Etoposide to PHB coated MNPs

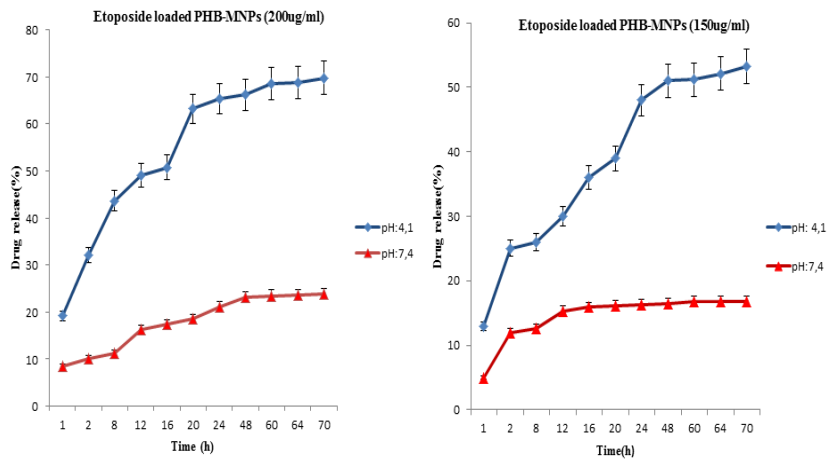


Fig 3. Drug release plot of Etoposide loaded PHB-coated iron oxide nanoparticles (at acidic (pH 4.1) and neutral (pH 7.4) pHs

In this study, after the characterization of PHB coated MNPs, Etoposide loading studies were done in pH 7.4 PBS buffer. In order to find maximum drug loading capacity on PHB coated MNPs, Etoposide concentration gradually increased up to 250 µg/mL where the loading efficiency started to decrease. The highest and most efficient drug loading concentration was obtained at 200 µg/ml. The loading efficiency of 200 µg/ml Etoposide was %70 in pH 7.4 PBS buffer (Fig 2).

The present study, the most efficiently loaded drug concentrations (150 and 200 mg/mL) were selected, and release studies were performed at pH 7.4 and 4.1. The release studies were continued up to 70 hours.

The released of siRNA-Etoposide loaded PHB coated MNPs was studied in pH 7.4 at 37°C because of mimics physiological conditions. In addition, the release of siRNA-Etoposide loaded PHB coated MNPs was studied in acetate buffer at pH 4.1 because of the acidic tumor microenvironment. The results showed that about 60% of the Etoposide released within 20 hours at pH 4.1. However, Etoposide released from Etoposide-loaded PHB-MNPs was more stable up to 70 hours at pH 7.4 (Fig 3).

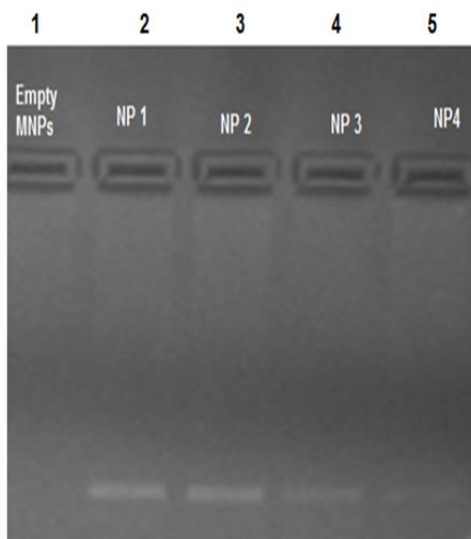


Fig 4. Agarose gel (1, 2%) of siRNA-Etoposide loaded MNPs (8:1, 4:1, 2:1 and 1:1 w/w ratios) complexes (lane 2–5)

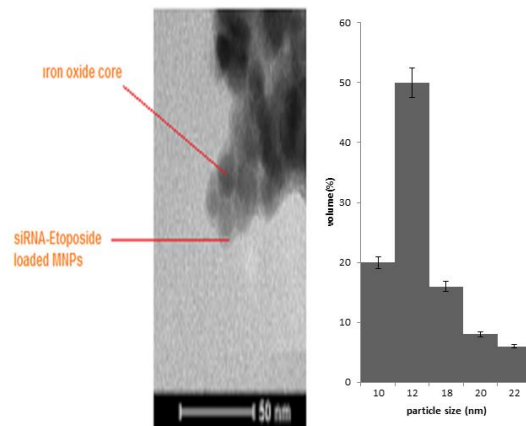


Fig 5. TEM image of siRNA-Etoposide loaded PHB-coated iron oxide nanoparticles

In addition, siRNA complex Etoposide-PHB-MNPs were studied on breast cancer cells and analyzed its therapeutic effectiveness (Fig 4). The size and morphological properties of siRNA-Etoposide loaded PHB-MNPs were observed through TEM image (Fig 5). According to the

scale bar on the TEM images of nanoparticles, the particle size of these nanoparticles was ranging between 10 and 22 nm. The cellular internalization of Etoposide- PHB-MNPs was identified by fluorescence microscopy (Fig 6).

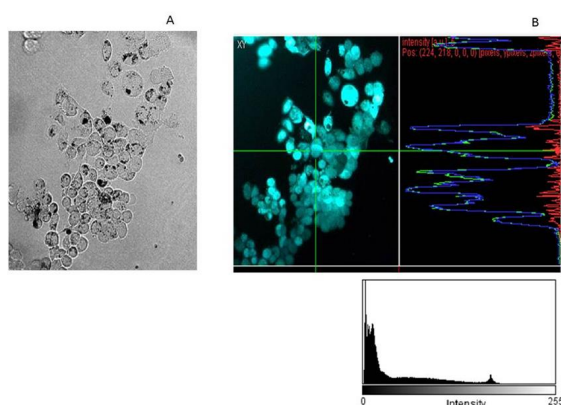


Fig 6. Cellular internalization of FITC conjugated magnetic nanoparticles by fluorescence microscopy (X40) (Fluorescence intensity graph of FITC conjugated Etoposide loaded magnetic nanoparticles)

In Fig 7 demonstrated that siRNA-Etoposide-PHB- MNPs were successfully received by cancer cells, even at low concentrations. The zeta potential values of PHB-MNPs were calculated as -11 mV in pH 7.4. The zeta potentials of siRNA-Etoposide-PHB-MNPs were observed at +19.1 mV. In addition, the size measurement of the particles was analyzed Dynamic light scattering and particles swelled. The average sizes of siRNA-Etoposide-PHB-MNPs were found as 100 nm in DLS measurements.

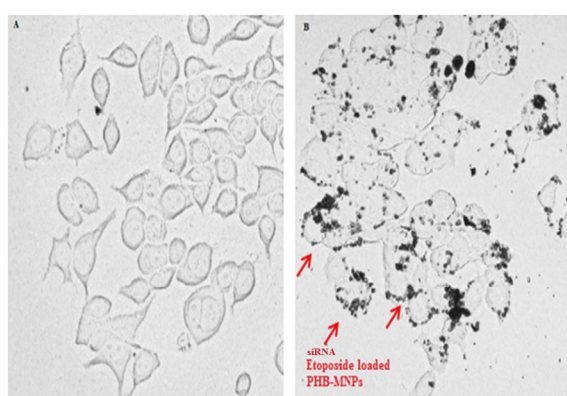


Fig 7. The internalization of siRNA-Etoposide loaded MNPs

Molecular docking analyses is a important tool of structure-based drug discovery to predict ligand-protein interaction and binding affinities using computation methods in the last decade

[76,77]. According to molecular docking results, the binding affinity of Etoposide(as control) and nanoparticle with drug were calculated to be (-9.1 kcal/mol and -10.4 kcal/mol, respectively). The 3D interaction diagrams are shown in Fig 8 and 9. The hydrogen-bonding interactions of Etoposide were observed with Glu 694 and Tyr710. The aminoacid residues of nanoparticles (one arm) with drug involved Trp710, Trp716, Trp653, Ser686. The drug loaded nanoparticle was designed as a single arm. The number of arms and binding energy are proportional. This part of the study is a preliminary study.

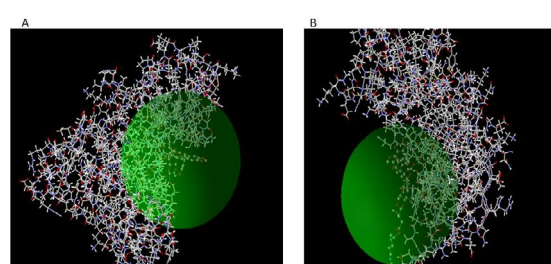


Fig 8. The 3D representation of etoposide (A) nanoparticles with drug (B) at the active site of human MRP1 protein in molecular docking

## DISCUSSION

Drug targeting strategies have been the area of extensive focus in cancer therapy. Recently, several drug delivery systems with nanoparticles [33-35] and techniques [36] were developed to boost the tumor reach of anticancer agents. Iron oxide-based nanoparticles have been commonly used for delivering anticancer agents to tumors [37, 38].

The short circulation time, the poor potential, retention in endosomes, toxicity on healthy cells are different limitations for conventional chemotherapeutic drugs. The nanoparticle-based drug delivery systems have shown promising efficacy compared with conventional chemotherapeutic drugs. At the present time, some nanoparticle formulations such as Albumin Paclitaxel Nanoparticle (Abraxane) for cancer treatment have been already approved by Food and Drug Administration (FDA). These intelligent drugs rise the intracellular concentration of their in cells while preventing toxicity to normal cells and use to overcome multidrug resistance.

The tumor microenvironment has some characteristics, including acidic pH [39-43], hypoxia[44-48], and enzymes[49-52]. The design pH sensitive nanoparticles have various properties in the molecular structure, pKa values

are close to the tumor interstitial pH. The tumor microenvironment have slightly acidic pH, when nanoparticle reach to tumor site, structure of nanoparticles is transformed with the change of pH, and then anticancer agent release from nanoparticle [53,54]. siRNA-Etoposide loaded PHB coated magnetic nanoparticles designed with a strong cationic structure will not be destroyed by enzymes until they reach the target cells. After the internalization of nanoparticles to the cell, the nanoparticle systems are designed to facilitate the release of siRNA depending on the intracellular pH. Major barriers in cancer treatment are MRP1 and P-gp that decrease the accumulation of drugs inside the cancer cells, have an important role in the development of resistance to anticancer drugs and overexpressed in different cancers [55]. To date, the anti-cancer drug-loaded nano-based therapeutic approaches have been proposed to have great potential in decreasing the mentioned troubles of cancer therapy [56-57].

The major problem in siRNA delivery systems is their deficiency to form condensed nanoparticles with polymers. This situation can form a very stable and condensed nanoparticle structure with cationic molecules. The siRNA is loosely connected to nanoparticles can be easily attacked by nucleases in the circulating systems and quickly degraded before arrival at the targeted tumor cells. The modification of cationic molecules for nanoparticle systems in gene delivery will benefit in their efficient therapeutics applications [58].

In this study, siRNA-Etoposide loaded MNPs were successfully taken up by cancer cells. In the literature, synthesized magnetic nanoparticles show some agglomeration similarly to this study [58-60]. In this study, because of the smaller particle sizes of nanoparticles have surface energy and very large surface area may increase the agglomeration. Before in vivo applications, the dissolving of polymer-coated MNPs with various solvents such as PBS, or ultrasonication may support to overcome the agglomeration problem. In addition, nanoparticle concentration is shown to be critical for agglomeration in studies [59-61]. After the uptake into the cells, the drug concentration can be enhanced significantly and nanoparticles play important role as drug store [6]. The cytotoxic effect of Etoposide-loaded PHB-MNPs, siRNA-Etoposide-PHB-MNPs on cancer cells was investigated by XTT assay, and IC50 values were calculated. In this study, empty PHB-

MNPs were not shown cytotoxic effect up to 500 mg/mL. Previously, Kaplan et al. [26] reported the IC50 value of MCF-7 and MCF-7/1000Eto cells were identified as 50,6  $\mu$ M and 135,7  $\mu$ M, respectively. MCF-7/1000Eto cells are 2.7 fold resistant to etoposide relative to parental MCF-7/S cell line. IC50 values of siRNA Etoposide loaded PHB-MNPs were identified as 10,18  $\mu$ M and 39,21  $\mu$ M on MCF-7 and MCF-7/1000 Eto cells, respectively. From the IC50 values, it was seen that the loading of siRNA-Etoposide-PHB-MNPs increased its efficiency nearly up to 3,5 fold on MCF-7/1000 Eto cancer cells.

Here we show that combined treatment of siRNA and Etoposide loaded PHB-MNPs is stronger suppression of MRP1 expression. To determine the effect of siRNA-etoposide MNPs, we investigated the expressions of MRP1 gene expression on MCF/7 and MCF-7/1000Eto. According to the gene expression results, MRP1 gene expression was 4 fold upregulated in MCF-7/1000Eto cells. However, it was about 3 fold downregulated due to the application of siRNA-Etoposide loaded magnetic nanoparticles.

## CONCLUSION

In this study, in order to research in vivo activity of siRNA-Etoposide loaded magnetic nanoparticles, MCF/7 and MCF-7/1000Eto was treated with siRNA-Etoposide loaded magnetic nanoparticles. The result showed that siRNA-Etoposide loaded magnetic nanoparticles can effectively inhibit cancer cells. The biologic and docking analyse results suggested that these nanoparticles the may be a novel candidate for drug resistance breast cancer therapy.

## FUNDING

The support of Kirsehir Ahi Evran University, Central Research and Application Laboratory for analyses is gratefully acknowledged, as well as financial support by Coordinatorship of SRP (FEF. E2.17.018).

## ACKNOWLEDGEMENTS

The support of Kirsehir Ahi Evran University, Central Research and Application Laboratory for analyses is gratefully acknowledged, as well as financial support by Coordinatorship of SRP (FEF. E2.17.018).

## REFERENCES

1.Clark PI, Slevin ML. The clinical pharmacology of etoposide

- and teniposide. *Clin Pharmacokinet.* 1987; 12(4): 223–252.
2. Chamberlain M. Recurrent brainstem gliomas treated with oral VP-16. *J Neurooncol.* 1993; 15(2): 133–139.
  3. Ashley DM, Meier L, Kerby T. Response of recurrent medulloblastoma to low-dose oral etoposide. *J Clin Oncol.* 1996; 14(6): 1922–1927.
  4. Shah JC, Chen JR, Chow D. Preformulation study of etoposide: identification of physicochemical characteristics responsible for the low and erratic oral bioavailability of etoposide. *Pharm Res.* 1989; 6(5): 408–412.
  5. Zhang T, Chen J, Zhang Y. Characterization and evaluation of nanostructured lipid carrier as a vehicle for oral delivery of etoposide. *Eur J Pharm Sci.* 2011; 43(3): 174–179.
  6. Lamprecht A, Benoit JP. Etoposide nanocarriers suppress glioma cell growth by intracellular drug delivery and simultaneous P-glycoprotein inhibition. *J Control Release.* 2006; 112(2): 208–213.
  7. Masquelier M, Zhou QF, Gruber A. Relationship between daunorubicin concentration and apoptosis induction in leukemic cells. *Biochem Pharmacol.* 2004; 67(6): 1047–1056.
  8. Varshosaz J, Hassanzadeh F, Sadeghi AH. Uptake of etoposide in CT-26 cells of colorectal cancer using folate targeted dextran stearate polymeric micelles. *Biomed Res Int.* 2014; 708593.
  9. Varthya M, Pawar H, Singh C. Development of Novel Polymer-Lipid Hybrid Nanoparticles of Tamoxifen: in vitro and in vivo Evaluation. *J Nanosci Nanotechnol.* 2016; 16(1): 253–260.
  10. Khodadust R, Unsoy G, Yalcin S. PAMAM dendrimer-coated iron oxide nanoparticles: synthesis and characterization of different generations. *J Nanopart Res.* 2013; 15: 1488.
  11. Gabizon AA. in: V. Torchilin (Ed.), *Nanoparticulates as Drug Carriers*, Imperial College Press, London. 2011.
  12. Lawrence MJ, Warisnoicharoen W. in: V. Torchilin (Ed.), *Nanoparticulates as Drug Carriers*, Imperial College Press, London. 2006.
  13. Mäder K. in: V. Torchilin (Ed.) *Nanoparticulates as Drug Carriers*, Imperial College Press, London. 2006.
  14. Yordanov G, Skrobanska R, Evangelatov A. Colloidal formulations of etoposide based on poly(butyl cyanoacrylate) nanoparticles: preparation, physicochemical properties and cytotoxicity. *Colloids Surf B Biointerfaces.* 2013; 101: 215–22.
  15. Callewaert M, Dukic S, Gulick L. Etoposide encapsulation in surface-modified poly(lactide-co-glycolide) nanoparticles strongly enhances glioma antitumor efficiency. *J Biomed Mater Res A.* 2012; 101(5): 1319–1327.
  16. Gaucher G, Poreba M, Ravenelle F. Poly(N-vinylpyrrolidone)-block-poly(D,L-lactide) as polymeric emulsifier for the preparation of biodegradable nanoparticles. *J Pharm Sci.* 2007; 96(7): 1763–1775.
  17. Kilicay E, Demirbilek M, Turk M, et al. Preparation and characterization of poly(3-hydroxybutyrate-co-3-hydroxyhexanoate) based nanoparticles for targeted cancer therapy. *Eur J Pharm Sci.* 2011; 44(3): 310–320.
  18. Poreba R, Gac P, Poreba M. Environmental and occupational exposure to lead as a potential risk factor for cardiovascular disease. *Environ Toxicol Pharmacol.* 2011; 31(2): 267–277.
  19. Yadav KS, Jacob S, Sachdeva G, et al. Intracellular delivery of etoposide loaded biodegradable nanoparticles: cytotoxicity and cellular uptake studies. *J Nanosci Nanotechnol.* 2011; 11(8): 6657–6667.
  20. Khajavinia A, Varshosaz J, Dehkordi AJ. Targeting etoposide to acute myelogenous leukaemia cells using nanostructured lipid carriers coated with transferrin. *Nanotechnology.* 2012; 23(40): 405101.
  21. Jinturkar KA, Anish C, Kumar MK. Liposomal formulations of Etoposide and Docetaxel for p53 mediated enhanced cytotoxicity in lung cancer cell lines. *Biomaterials.* 2012; 33(8): 2492–2507.
  22. Varshosaz J, Hasanzadeh F, Eslamdoost M. Optimization of self-assembling properties of fatty acids grafted to methoxy poly(ethylene glycol) as nanocarriers for etoposide. *Acta Pharm.* 2012; 62(1): 31–44.
  23. Xiong YC, Yao YC, Zhan XY. Application of polyhydroxyalkanoates nanoparticles as intracellular sustained drug-release vectors. *Biomater Sci Polym Ed.* 2010; 21(1): 127–140.
  24. Yalcin S, Khodadust R, Unsoy G, et al. Synthesis and characterization of Poly-hydroxybutyrate (PHB) coated magnetic nanoparticles: toxicity analyses on different cell lines. *Inorganic and Nano-Metal Chemistry.* 2015; 45(5): 700–708.
  25. Su Z, Liu G, Fang T. Silencing MRP1-4 genes by RNA interference enhances sensitivity of human hepatoma cells to chemotherapy. *Am J Transl Res.* 2016; 8(6): 2790–2802.
  26. Kaplan E, Gunduz U. Expression analysis of TOP2A, MSH2 and MLH1 genes in MCF7 cells at different levels of etoposide resistance. *Biomed Pharmacother.* 2012; 66(1): 29–35.
  27. Livak KJ, Schmittgen TD. Analysis of Relative Gene Expression Data Using Real-Time Quantitative PCR and the 2- $\Delta\Delta$ CT Method. *Methods.* 2001; 25(4): 402–408.
  28. Morris GM, Goodsell DS, Halliday RS, Huey R, Hart WE, Belew RK, Olson AJ (1998). Automated docking using a Lamarckian genetic algorithm and an empirical binding free energy function. *J Comput Chem.* 19(14): 1639–1662.
  29. Trott O, Olson AJ (2010). AutoDock Vina: improving the speed and accuracy of docking with a new scoring function, efficient optimization, and multithreading. *J Comput Chem.* 31 (2): 455e461.
  30. Ramaen O, Leulliot N, Sizun C, Ulryck N, Pamlard O, Lallemand JY, Tilbeurgh Hv, Jacquet E (2006). Structure of the human multidrug resistance protein 1 nucleotide binding domain 1 bound to Mg<sup>2+</sup>/ATP reveals a non-productive catalytic site. *J Mol Biol.* 359(4):940-9.
  31. Frisch, M. J., Trucks, G. W., Schlegel, H. B., Scuseria, G. E., Robb, M. A., Cheeseman, J. R., ... & Nakatsuji, H. (2009). Gaussian09 Revision D. 01, Gaussian Inc. Wallingford CT.
  32. Thomsen R, Christensen, MH (2006). MolDock: a new technique for high-accuracy molecular docking. *J Med Chem.* 49(11):3315-3321.
  33. Nomura T, Saikawa A, Morita S. 1998. Pharmacokinetic characteristics and therapeutic effects of mitomycin C-dextran conjugates after intratumoral injection. *J Control Release.* 1998; 52(3): 239–252.
  34. Maeda H, Sawa T, Konno T. Mechanism of tumor-targeted delivery of macromolecular drugs, including the EPR effect in solid tumor and clinical overview of prototype polymeric drug SMANCS. *J Control Release.* 2001; 74(1–3): 47–61.
  35. Yalcin S, Unsoy G, Mutlu P, et al. Polyhydroxybutyrate coated magnetic nanoparticles for Doxorubicin delivery: Cytotoxic effect against Doxorubicin-resistant breast cancer cell line. *Am J Ther.* 2014; 21(6): 453–461.
  36. Marin A, Sun H, Husseini GA. Drug delivery in pluronic

- micelles: effect of high-frequency ultrasound on drug release from micelles and intracellular uptake. *J Control Release*. 2002;84(1-2): 39-47.
37. Williams J, Lansdown R, Sweitzer R. Nanoparticle drug delivery system for intravenous delivery of topoisomerase inhibitors. *J Control Release*. 2003; 91(1-2): 167-172.
  38. Harivardhan RL, Sharma RK, Chuttani K, et al. Influence of administration route on tumor uptake and biodistribution of etoposide loaded solid lipid nanoparticles in Dalton's lymphoma tumor bearing mice. *J Control Release*. 2005; 105(3): 185-98.
  39. Xia F, Hou W, Zhang Cl. pH-responsive gold nanoclusters-based nanoprobe for lung cancer targeted near-infrared fluorescence imaging and chemo-photodynamic therapy. *Acta Biomaterialia*. 2018; 68: 308-319.
  40. Hao Y, Zheng C, Wang L et al. 2017. Tumor acidity-activatable manganese phosphate nanoplateform for amplification of photodynamic cancer therapy and magnetic resonance imaging. *Acta Biomater*. 2017; 62: 293-305.
  41. Shi XX, Ma X, Hou M, et al. pH-responsive unimolecular micelles based on amphiphilic star-like copolymers with high drug loading for effective drug delivery and cellular imaging. *J Mater Chem B*. 2017; 5: 6847-6859.
  42. Lin WJ, Yao N, Qian L. pH-responsive unimolecular micelle-gold nanoparticles-drug nanohybrid system for cancer theranostics. *Acta Biomater*. 2017; 58: 455-465.
  43. Fang S, Lin J, Li C et al. Dual-stimuli responsive Nanotheranostics for multimodal imaging guided Trimodal synergistic therapy. *Small*. 2017;13(6).
  44. Du J, Lane LA, Nie S. Stimuli-responsive nanoparticles for targeting the tumor microenvironment. *J Control Release*. 2015;219: 205-214.
  45. Chen Q, Feng LZ, Liu JJ. 2016. Intelligent albumin-MnO<sub>2</sub> nanoparticles as pH-/H<sub>2</sub>O<sub>2</sub>-responsive dissociable Nanocarriers to modulate tumor hypoxia for effective combination therapy. *Adv Mater*. 2016; 28(33): 7129-7136.
  46. Feng LL, Gai S, He F. Controllable generation of free radicals from multifunctional heat-responsive Nanoplateform for targeted cancer therapy. *Chem Mater*. 2018; 30(2): 526-539.
  47. Yang GB, Zhang R, Liang C. Manganese dioxide coated WS<sub>2</sub>@Fe<sub>3</sub>O<sub>4</sub>/sSiO<sub>2</sub> Nanocomposites for pH-responsive MR imaging and oxygen-elevated synergetic therapy. *Small*. 2018; 14(2).
  48. Cho MH, Choi ES, Kim S, Goh SH, Choi Y. Redox-responsive manganese dioxide nanoparticles for enhanced MR imaging and radiotherapy of lung cancer. *Front Chem*. 2017; 5: 109.
  49. Moreira AF, Dias DR, Correia IJ. Stimuli-responsive mesoporous silica nanoparticles for cancer therapy: a review. *Micropor Mesopor Mat*. 2016; 236: 141-157.
  50. Hu QY, Katti PS, Gu Z. Enzyme-responsive nanomaterials for controlled drug delivery. *Nanoscale*. 2014; 6(21): 12273-12286.
  51. Li JM, Liu F, Shao Q, Min YZ, et al. Enzyme-responsive cell-penetrating peptide conjugated Mesoporous silica quantum dot Nanocarriers for controlled release of nucleus-targeted drug molecules and real-time intracellular fluorescence imaging of tumor cells. *Adv Healthc Mater*. 2014; 3(8): 1230-1239.
  52. de la Rica R, Aili D, Stevens MM. Enzyme-responsive nanoparticles for drug release and diagnostics. *Adv Drug Deliver Rev*. 2012; 64(11): 967-978.
  53. John JV, Uthaman S, Augustine R, et al. pH/redox dual stimuli-responsive sheddable nanodisks for efficient intracellular tumour-triggered drug delivery. *J Mater Chem B*. 2017;5(25): 5027-5036.
  54. Uthaman S, Huh K, Park IK. Tumor microenvironment responsive nanoparticles for cancer theragnostic applications. *Biomater Res*. 2018; 22:22.
  55. Hande KR. Etoposide: four decades of development of a topoisomerase II inhibitor. *Eur J Cancer*. 1998; 34(10): 1514-1521
  56. Lundstrom K. Cancer therapy applying viral nanoparticles. In: Khudyakov Y, Pumpens P, editors. *Viral Nanotechnology*. Boca Raton: Taylor & Francis 2015; 455-466.
  57. Baker JR. Dendrimer-based nanoparticles for cancer therapy. *Hematology Am Soc Hematol Educ Program*. 2009; 708-719.
  58. Lee SJ, Huh MS, Lee SY, Min S, Lee S, Koo H, Chu JU, Lee KE, Jeon H, Choi Y, Choi K, Byun Y, Jeong SY, Park K, Kim K, Kwon IC. Tumor-homing poly-siRNA/glycol chitosan self-cross-linked nanoparticles for systemic siRNA delivery in cancer treatment. *Angew Chem Int Ed Engl*. 2012 Jul 16; 51(29): 7203-7207.
  59. Predescu AM, Matei E, Berbecaru AC, Pantilimon C, Drăgan C, Vidu R, Predescu C, Kuncser V. Synthesis and characterization of dextran-coated iron oxide nanoparticles. *R Soc Open Sci*. 2018; 5(3): 171525.
  60. Dung DTK, Hai TH, Phuc LH, Long BD, Vinh LK, Truc PN. Preparation and characterization of magnetic nanoparticles with chitosan coating. *APCTP-ASEAN Workshop on Advanced Materials Science and Nanotechnology (AMSN08) IOP Publishing Journal of Physics: Conference Series*. 2009; 187: 012036
  61. Zhang XL, Niu HY, Zhang SX, Cai YQ. Preparation of a chitosan-coated C18-functionalized magnetite nanoparticle sorbent for extraction of phthalate ester compounds from environmental water samples. *Anal Bioanal Chem*. 2010b; 397: 791-798.